# Numerical Study of the Seasonal Variations of the Subtropical Front and the Subtropical Countercurrent

KENSUKE TAKEUCHI

*Department of Geophysics, Hokkaido University, Sapporo, 060 Japan*

(Manuscript received 1 July 1985, in final form 21 November 1985)

ABSTRACT

Response of the Subtropical Countercurrent and the Subtropical Front in the North Pacific Ocean to seasonally changing wind stress and thermal condition are examined using the same idealized numerical model that the author used in 1984 for steady state modeling of the Subtropical Countercurrent and the Subtropical Front. The model reproduces the main features of the observed seasonal variations reasonably well, especially that the Subtropical Countercurrent is strong in spring and weak in fall. It is also shown that the seasonal variation of wind stress and thermal condition intensifies the annual mean strength of the Subtropical Countercurrent.

The relative importance of the seasonal variations of wind stress and thermal condition is examined using models in which only one of these changes and the other is fixed. The results indicate that the seasonal variation of the Subtropical Countercurrent is mainly due to the seasonal change of wind stress, while the seasonal change of thermal condition is mostly responsible for the intensification of the annual mean of the Subtropical Countercurrent and the Subtropical Front.

## 1. Introduction

It is not very clear how far back we must search to find the first literature describing the seasonal variation of the Subtropical Front or the Subtropical Countercurrent. Uda and Hasunuma (1969) pointed out that in the western North Pacific the upper portion of the Subtropical Front shifts farther north in the seasons from late spring to fall, while the subsurface portion remains almost at the same position in all seasons. Roden (1975) reported that the surface portion of the Subtropical Front remains only as a salinity front from summer to fall. Similar seasonal changes in the surface portion of the Subtropical Front can be seen in the monthly zonal temperature cross sections of the North Atlantic by Schroeder (1965).

More quantitative analyses were done by White et al. (1978) for the western North Pacific. They compiled all available hydrographic data over a 20-year period, on a 2.5° latitude by 5.0° longitude grid, and made monthly mean maps of the temperature and zonal relative geostrophic flow (0/200 db). Figure 1, copied from their paper, shows the seasonal variation of the strength and latitudinal position of the Subtropical Countercurrent. The main features which can be found in this figure are as follows.

1) The Subtropical Countercurrent is strong in spring and weak in fall.

2) The amplitude of the seasonal variation in strength of the Subtropical Countercurrent is larger in the region close to the western boundary.

3) The Subtropical Countercurrent is located at a higher latitude from winter to spring in the region close to the western boundary, while no systematic seasonal change in location is seen far from the western boundary.

To date, no theory exists to explain the cause of these seasonal variations. Also, the relationship between the features mentioned and the northward shift of the surface portion of the Subtropical Front shown by Uda and Hasunuma (1969) is not clear.

Takeuchi (1984) made a simple, steady state numerical model of the North Pacific Ocean, and succeeded in reproducing the Subtropical Front and the Subtropical Countercurrent. In the present study, the same model ocean is used to examine the response of the Subtropical Countercurrent and the Subtropical Front to the seasonal change of the wind stress and/or the thermal conditions at the sea surface. As the seasonal variations are important properties of the Subtropical Countercurrent and the Subtropical Front, a model for the Subtropical Countercurrent and the Subtropical Front can be said to be truly valid only if their seasonal variations are represented well in the model. This is the main motivation for the present study. Hereinafter, the steady model used in the previous study (Takeuchi, 1984) is referred to as the basic model.

The definition of the "Subtropical Front" and the "Subtropical Countercurrent" differ slightly among different authors. In the present paper, the Subtropical Countercurrent is used as the eastward current associated with the Subtropical Front.

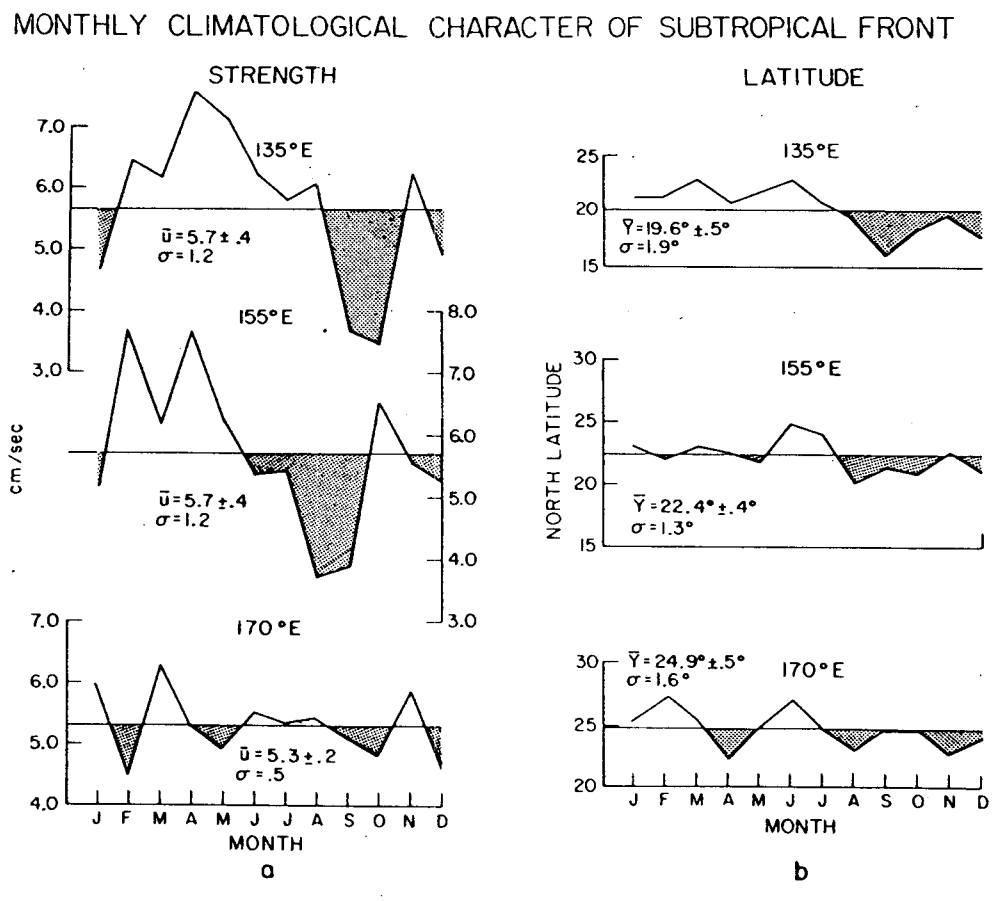


FIG. 1. Indices of (a) the monthly long-term mean strength and (b) the latitudinal position of the Subtropical Front at three longitudes. (From White et al., 1978.)

## 2. Model

The model ocean and the governing equations are the same as in the basic model, so they are described only briefly here. More detailed descriptions are found in Takeuchi (1984). The model ocean is a rectangular basin with a flat bottom, whose dimensions are 4900 km, 7800 km and 5200 m in meridional, zonal and vertical directions, respectively (Fig. 2). The Coriolis parameter is zero at the southern boundary (corresponding to the equator) and increases linearly to the north. Only density is used directly as a thermodynamic variable, instead of temperature and salinity. The model is based on the hydrostatic, Bousinesq and rigid-lid approximations. Convective adjustment is employed to maintain a statically stable stratification. The main parameters used in the model are shown in Table 1.

The buoyancy flux through the sea surface is determined by the following formula (Haney, 1971),

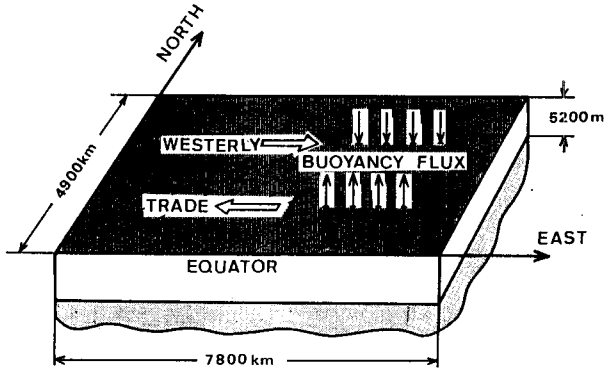


FIG. 2. Schematic diagram of the model ocean.

TABLE 1. Main parameters used in the model.

| | | |
|---|---|---|
| Meridional gradient of Coriolis parameter | | $\beta = 2.0 \times 10^{-13}$ cm$^{-1}$ s$^{-1}$ |
| Coefficient of eddy diffusivity | lateral | $K_H = 1.0 \times 10^{7}$ cm$^2$ s$^{-1}$ |
| | vertical | $K_V = 1.0$ cm$^2$ s$^{-1}$ |
| Coefficient of eddy viscosity | lateral | $A_H = 1.0 \times 10^{9}$ cm$^2$ s$^{-1}$ |
| | vertical | $A_V = 10.0$ cm$^2$ s$^{-1}$ |
| Grid interval | meridional | $\Delta Y = 160$ km |
| | zonal | $\Delta x = 320$ km |
| Number of levels in vertical | | $K = 10$ |

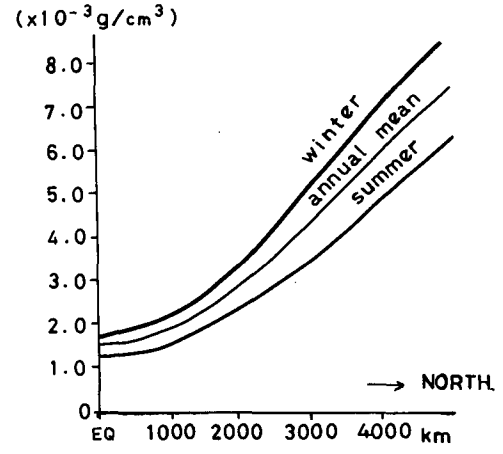


FIG. 3. Distribution of $\rho_a$ in each season. The distribution for spring and fall is the same as for the annual mean.

$$Q = \text{const} \times (\rho_a - \rho_s),$$

where $Q$ is the buoyancy flux, $\rho_s$ is the density of the water at the sea surface, and $\rho_a$ is a given function of latitude and time. Corresponding to the seasonal change of the thermal conditions, $\rho_a$ changes sinusoidally in time, with the period of one year: larger (corresponding to colder) in winter and smaller (warmer) in summer (Fig. 3). The amplitude of the seasonal change of $\rho_a$ is larger at higher latitudes, corresponding to the observational fact that the seasonal variations of the thermal conditions are larger at higher latitudes.

Observations show strong seasonal variations in both zonal and meridional components of wind stress, especially near the western and eastern boundaries. However, as the Subtropical Front and the Subtropical Countercurrent are successfully reproduced using only the zonal component of wind stress in the basic model, and it is desirable to keep the model simple, only the zonal component of wind stress is included as a first-order approximation. The wind stress is only dependent on latitude and time. Figure 4 shows the observed wind stress averaged in the zonal direction (Kutsuwada, 1982). The main features, especially in the Subtropical Gyre, are as follows.

1) The wind stress curl is stronger in winter.
2) The region where the wind stress curl is negative shifts northward in summer.

The model wind stress is designed to include these features:

1) The annual mean wind stress is identical to that of the basic model.
2) Wind stress changes sinusoidally in time at each latitude with a period of one year.
3) The phase of the seasonal change of wind stress in the poleward portion of the model ocean leads that in the equatorward portion by 2.4 months.

The latitudinal distribution of the model wind stress in each season is shown in Fig. 5.

Three model experiments are made. In Model D1, both wind stress and surface thermal condition change, and in D2 and D3, only one of them changes. The purpose of D2 and D3 is to obtain some information about the individual roles of the seasonal variations of the wind and the thermal condition.

In all of these experiments we use the result of the basic model as the initial condition. The integration is carried out for about 20 years in each experiment, and a quasi-steady periodic state is attained.

In the present study, the artificial speeding-up method—proposed by Bryan et al. (1975) and used in the basic model—is not employed. Otherwise, the scheme for the numerical calculation is the same as the one used in the basic model.

## 3. Result

First we describe the results of Model D1. The horizontal distributions of current and density in each season are shown in Fig. 6. The seasonal variations are not clearly seen in this figure except in the equatorial region, where the internal Rossby waves have the larger phase speed and the response of the ocean to the change of the wind stress is quicker. In order to see the seasonal variations of the Subtropical Countercurrent, the maximum speed of the Subtropical Countercurrent (zonal component) and latitudinal position of the maximum

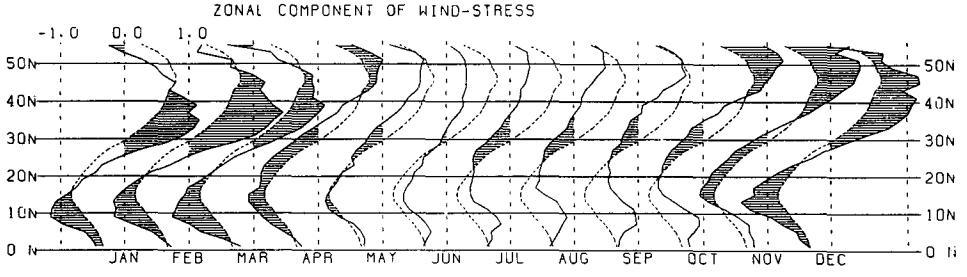


FIG. 4. Annual cycle of meridional profiles of the zonal component of wind stress zonally averaged over the Pacific Ocean. Solid lines show monthly mean and dashed lines, annual mean. (From Kutsuwada, 1982.)

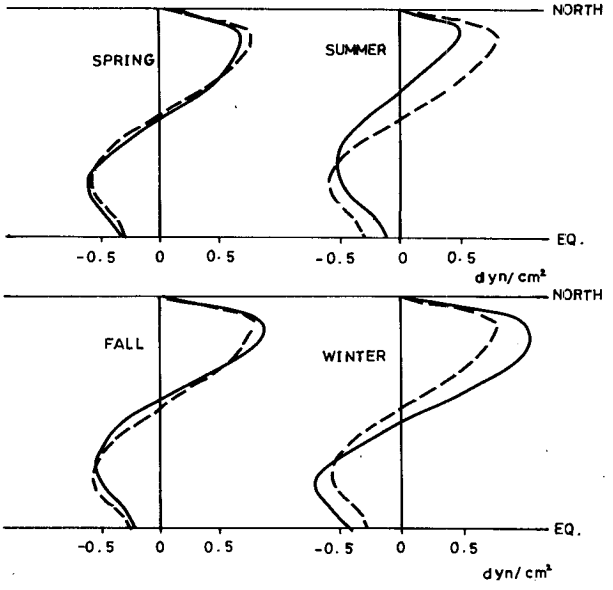


FIG. 5. Meridional distribution of zonal wind stress in each season used in models D1 and D2. Dashed line shows the annual mean.

at some longitudes are shown and compared to those of the basic model (shown by dashed lines) in Fig. 7. The seasonal changes in position are not significant considering the meridional grid size (160 km) used in the model. However, as the changes are smooth and systematic, it is suggested that the seasonal change of the location shown in Fig. 7 is not without meaning.

The major conclusions are as follows.

1) The strength and position of the Subtropical Countercurrent varies nearly sinusoidally in time with a period of one year (i.e., only the variation that has the same cycle as the variations of the external conditions is significant).

2) The Subtropical Countercurrent is strong in spring and weak in fall.

3) The amplitudes of the seasonal variation both in strength and position are larger in the region closer to the western boundary.

4) The seasonal change in position is almost out of phase between the region close to the western boundary and the eastern region. In the region close to the western boundary the Subtropical Countercurrent shifts northward in the season from winter to spring.

5) The annual mean strength of the Subtropical Countercurrent is about 1 cm $s^{-1}$ stronger than that of the basic model.

Comparison of these results with the analyses by White et al. (1978) shows that in the region close to the western boundary, both strength and latitudinal position of the Subtropical Countercurrent agree well.

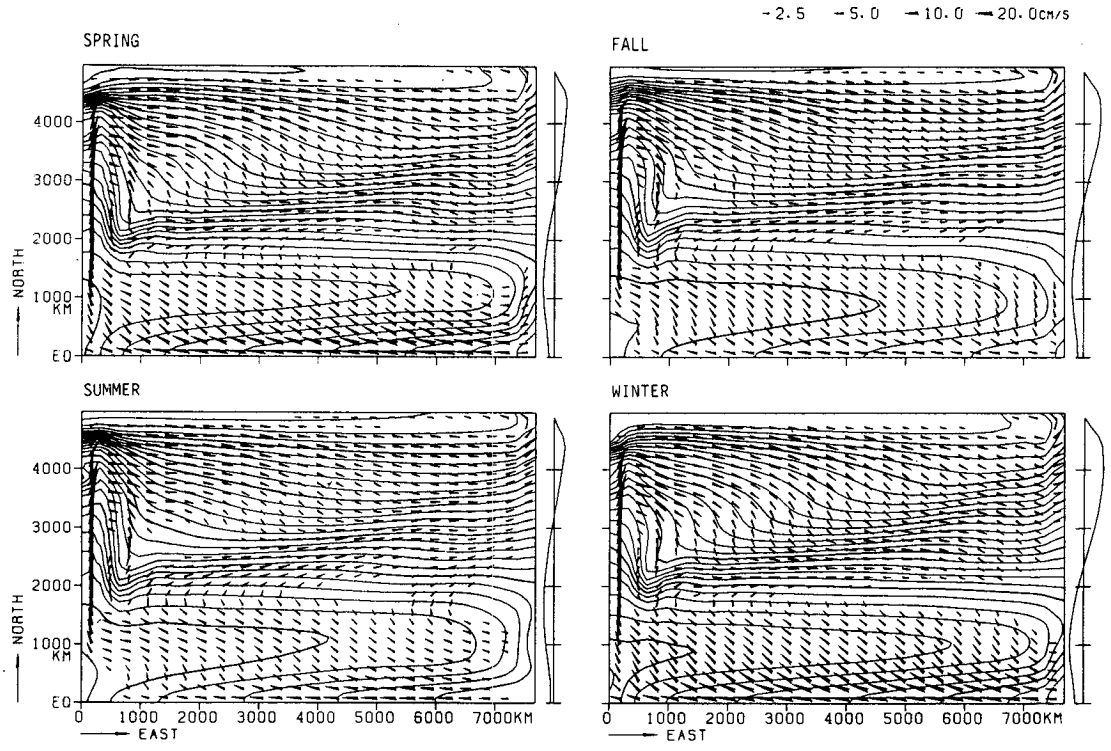


FIG. 6. Horizontal distribution of density (contoured every $2.0 \times 10^{-4}$ g $cm^{-3}$) and current at the sea surface in each season. Wind stress at each season is shown on the right of each panel.

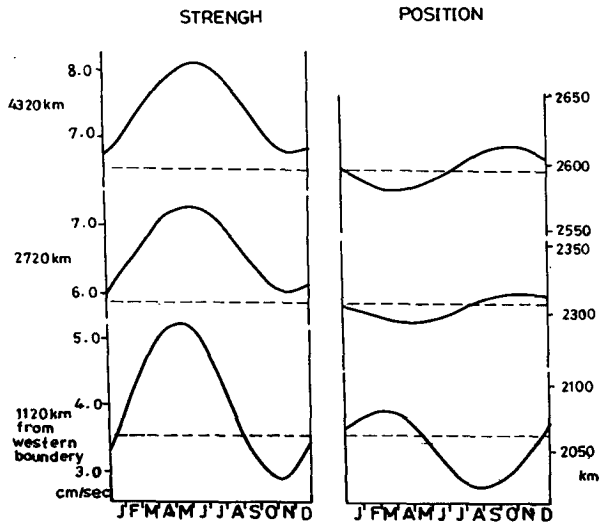


FIG. 7. Seasonal variation of the maximum speed (in $cm^{-1}$ s) and location of the Subtropical Countercurrent in Model D1 at (top to bottom) 4320 km, 2720 km and 1120 km from the western boundary. Dashed lines show the values in the basic model.

The tendency that the seasonal variation of the Subtropical Countercurrent is more significant in the region closer to the western boundary also agrees qualitatively. Observations show that the seasonal variation is not significant at 170°E, but in the model the seasonal variation is clearly seen even in the eastern part. However, considering a possibility that in observations seasonal signals are masked by shorter time-scale variations or sampling noises, this disagreement does not entirely deny the results of the model. In total, it can be said that the agreement between the model and observation is reasonably good.

A typical seasonal variation of the front structure can be seen in Fig. 8, where the meridional density distribution and circulation of four seasons are shown. Considerable differences between seasons are found in the surface layer, while the subsurface portion of the ocean does not show marked seasonal changes. In summer and fall, a seasonal thermocline is formed over the northern portion of the Subtropical Gyre and the isotherms, which intersect the ocean surface above the subsurface front in spring and winter, intersect the ocean surface at much higher latitudes. As a consequence, the surface front disappears from the area where it is found in spring and winter. As mentioned previously, such phenomena are also observed in the real ocean. However, as the location of the axis of the Subtropical Countercurrent coincides with the subsurface front regardless of the disappearance of the surface front as seen in Fig. 7, a strong relation is indicated between the Subtropical Countercurrent and the subsurface front.

The seasonal variations in strength and position of the Subtropical Countercurrent in Model D2 and D3 are shown in Fig. 9, along with the result of D1. The results suggest the following. The seasonal variation of the wind stress is the main cause of the seasonal variation of the strength of the Subtropical Countercurrent, while the seasonal variation of the thermal condition is more responsible for the mean intensification of the Subtropical Countercurrent. For seasonal change of the position of the Subtropical Countercurrent, the seasonal change of wind stress is more effective.

## 4. Discussion

First, we discuss the reason why the Subtropical Countercurrent is strong in spring and weak in fall. The wind stress and the thermal condition have only slight difference between spring and fall in Model D1. As the Subtropical Countercurrent is driven by concurrence of the wind-driven circulation and the differential heating (Takeuchi, 1984), the Subtropical Countercurrent is expected to be stronger when the wind stress or the differential heating is stronger. Hence we may expect that winter is the preferred season for the Subtropical Countercurrent to be strong. In steady state models with forcing corresponding to the condition of each season, the Subtropical Countercurrent is strongest in a model with winter conditions and weakest in a model with summer conditions. However, the Subtropical Countercurrent is strong in spring and weak in fall in the seasonal variation model. This indicates a phase lag of one season.

In an attempt to explain the phase lag, a simple "toy" model is made. Let $U_e$ be the strength of the Subtropical Countercurrent at the final steady state if the external condition is fixed. Thus, it is a function of the external condition. The strength of the Subtropical Countercurrent, $U$, is expected to approach $U_e$, and as the first-order approximation, assume that the rate of the approach is proportional to the difference between $U$ and $U_e$, as in (1):

$$\frac{dU}{dt} = c(U_e - U). \tag{1}$$

Then assume the external condition changes in such a way so that $U_e$ changes sinusoidally in time as follows:

$$U_e = a\cos\omega t. \tag{2}$$

Then Eq. (1) has a solution of the form:

$$\left.\begin{aligned} U &= \frac{ac}{(\omega^2 + c^2)^{1/2}}\cos(\omega t - \phi) \\ \phi &= \arctan\frac{\omega}{c} \end{aligned}\right\} -\frac{\pi}{2} \leqslant \phi \leqslant \frac{\pi}{2}. \tag{3}$$

This solution indicates that when the response time of the Subtropical Countercurrent ($1/c$) is much longer than one year, the phase lag of the response approaches a quarter-year. An experiment was performed in which the external conditions were changed abruptly, and the

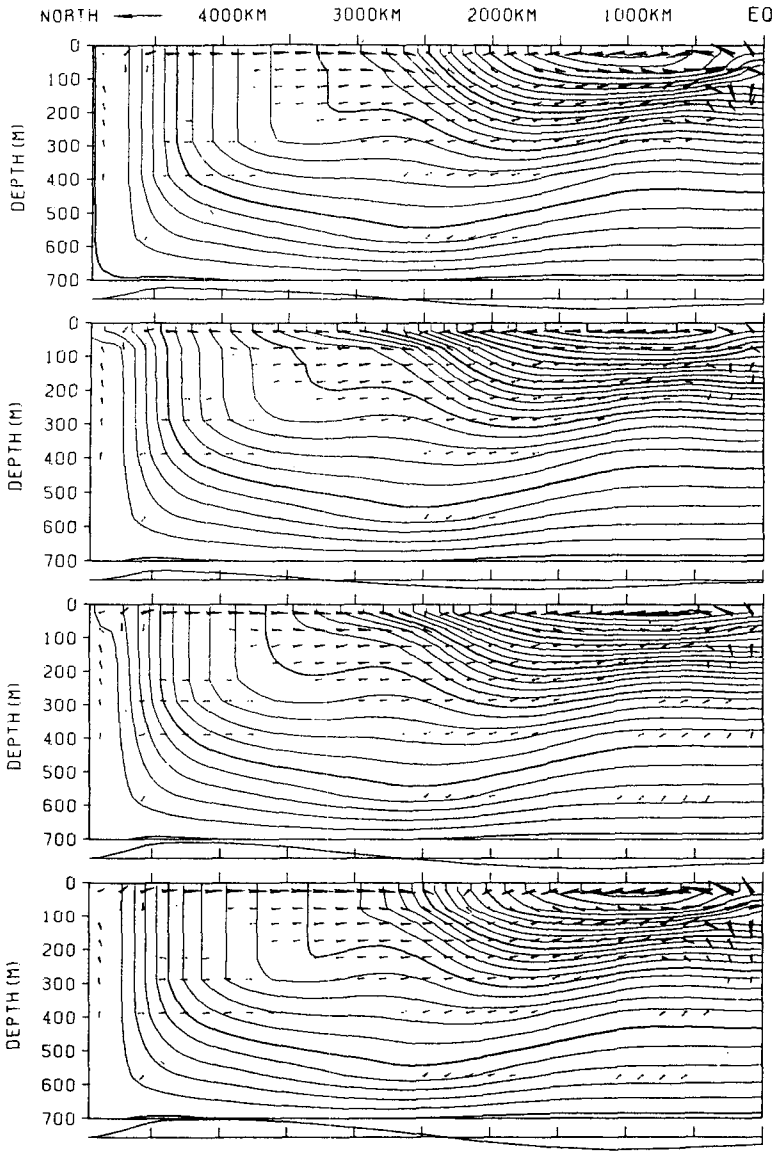


FIG. 8. Distribution of density and current in the meridional section (2720 km from the western boundary) in each season (top to bottom) spring, summer, fall and winter. The distribution of wind stress in each season is shown at the bottom of each panel.

results showed that the response of the Subtropical Countercurrent can be roughly approximated by Eq. (1) and that the response time is much longer than one year. However, this only explains the phase lag phenomenologically. The detailed mechanism, including the factor determining the response time, is left for future work. The response time may be related to travel time for a water particle to circulate in the Subtropical Gyre, because the results of the abrupt change model showed that the response time for the eastern portion of the Subtropical Countercurrent (i.e., outerward in the Subtropical Gyre) was longer.

The mechanism behind the seasonal variations of the position of the Subtropical Countercurrent is not clear. A possible candidate is the north–south migration of the Ekman convergence, which shifts poleward in summer and equatorward in winter. If it is true, a discussion analogous to the previous one for the strength of the Subtropical Countercurrent indicates that the latitude of the current axis should be highest between summer and fall. This agrees with the model results in the eastern part of the basin but disagrees with the model results near the western boundary (Fig. 7). This suggests that zonal wave propagation may be involved in addition to local forcing. This problem is also left for future work.

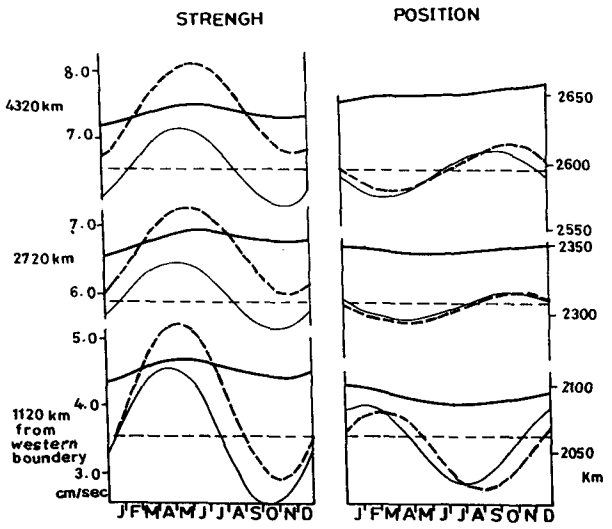


FIG. 9. As in Fig. 7, but for Models D2 (thin solid line) and D3 (thick solid line), along with Model D1 (thick dashed line) and the basic model (thin dashed line)

The seasonal variation of the wind and the thermal condition are important not only as the cause of the seasonal variations of the Subtropical Countercurrent, but also because they intensify the Subtropical Countercurrent in the annual mean. Figure 10 shows the differences in density and current distributions between the annual mean of Model D1 and the basic model. The Subtropical Countercurrent is markedly intensified compared to other currents.

The difference in the density distribution suggests the reason why the Subtropical Countercurrent is intensified. It is found that the poleward density gradient is greater in model D1, except in the surface layer. This is due to the difference between the effect of buoyancy sources and sinks. A buoyancy sink (analogous to surface cooling) reaches deep by convection, while the effect of a buoyancy source (surface warming) remains in the surface layer because it inhibits convection. Hence, for the ocean interior, the minimum surface density (given in winter) is most effective in determining the mean poleward density gradient. The seasonal change in $\rho_a$ is stronger in the north than in the south, as the seasonal change in $\rho_a$ is imposed to be larger in the north. This means that the poleward density gradient is virtually stronger in the seasonal variation model. Consequently, the Subtropical Front and the Subtropical Countercurrent are intensified in models D1 and D3.

## 5. Summary and conclusion

The main results of the seasonal variation model experiments in the present study can be summarized as follows.

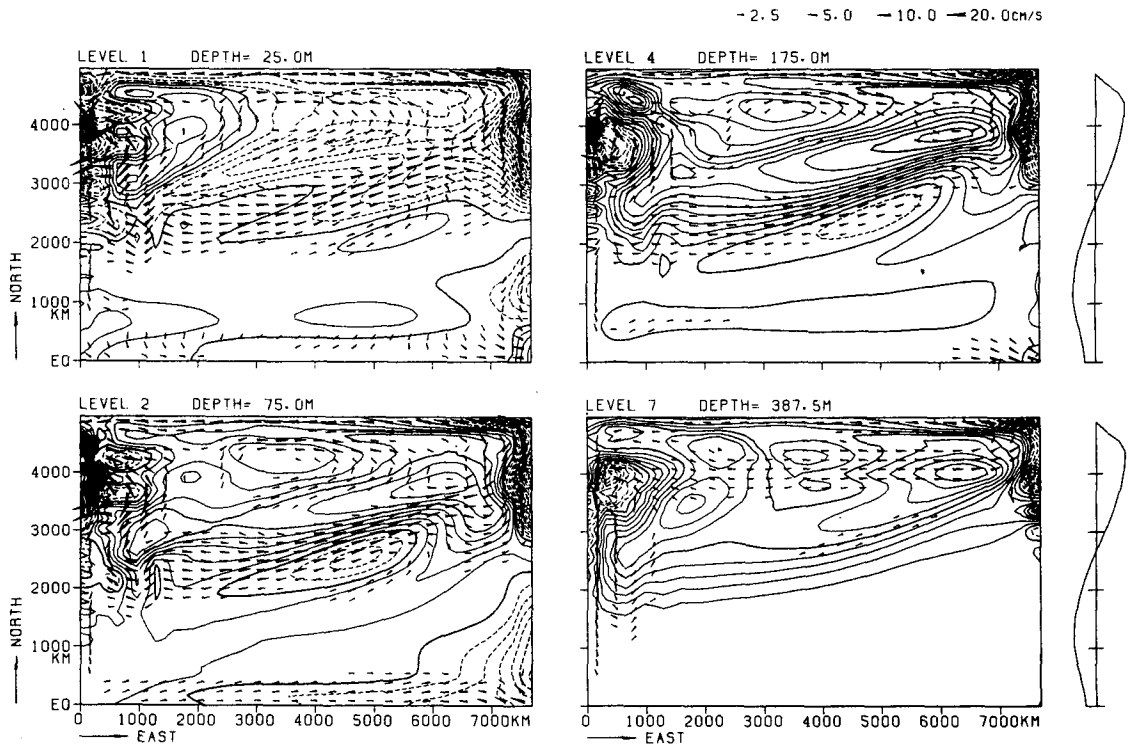


FIG. 10. Difference of the annual mean of Model D1 from the basic model. The values are enlarged (compared to Fig. 6) by a factor of 10. Solid lines indicate that the density is larger in the annual mean of Model D1.

1) The Subtropical Countercurrent is strong in spring and weak in fall.

2) The surface portion of the Subtropical Front exists near its location in the basic model, but it disappears from there in summer and fall.

3) The seasonal variation in strength of the Subtropical Countercurrent is mainly due to the seasonal change of wind stress.

4) The annual mean strength of the Subtropical Countercurrent is intensified in the seasonal variation model, and this intensification is mainly due to seasonal variation of the surface density condition.

Among these, results 1 and 2 show good agreement with observations, and no significant disagreement is found between the model and observations. Considering the simplicity of the present model, it is rather surprising that the main features of the seasonal variations of the Subtropical Countercurrent and the Subtropical Front are reproduced so well. It is suggested that result 3 can be explained by a phase lag due to the long response time of the Subtropical Countercurrent to change of the wind stress, compared to the time scale of the seasonal variation (1 year). Result 4 may be explained by the difference between the effects of buoyancy sources and sinks at the surface. This result should be emphasized as an interesting example showing that the seasonal variation cannot be neglected even when only the annual mean is of interest. At the same time, many questions are left for future work. One of them is the mechanism responsible for seasonal variation of the latitudinal location of the Subtropical Front and the Subtropical Countercurrent.

Although the present model is designed for the North Pacific Ocean, the model is idealized highly enough to be applicable to other oceans. Unfortunately, however, quantitative analyses of the seasonal variation of the Subtropical Countercurrent or the Subtropical Front are not available even for the North Atlantic Ocean. In most other oceans, their existence is unknown. Hopefully, altimetric data from satellite or XBT data from ships of opportunity should improve data availability for remote areas in the near future.

*Acknowledgments.* This paper would not have been finished without the various helpful suggestions, support and encouragement from the late Dr. Kozo Yoshida and Drs. Nobuo Suginahara, Benoit Cushman-Roisin, James O'Brien, Keiichi Hasunuma, Toshihiko Teramoto, Seiichi Kanari and many others. Miss Chikako Imai helped the author in drawing the figures. Comments and suggestions from the editor and reviewers were very helpful for the improvement of this paper. The author expresses heartfelt thanks to all of these people.

## REFERENCES

Bryan, K., S. Manabe and R. Pacanowski, 1975: A global ocean-atmosphere climate model. Part II: The ocean circulation. *J. Phys. Oceanogr.*, **5**, 30–46.

Haney, R. L., 1971: Surface thermal condition for ocean circulation models. *J. Phys. Oceanogr.*, **1**, 241–248.

Kutsuwada, K., 1982: New computation of the wind stress over the North Pacific Ocean. *J. Oceanogr. Soc. Japan*, **38**, 159–171.

Roden, G. I., 1975: On North Pacific temperature, salinity, sound velocity and density fronts, and their relation to the wind and energy flux field. *J. Phys. Oceanogr.*, **5**, 557–571.

Schroeder, E. H., 1965: Average monthly temperatures in the North Atlantic Ocean. *Deep Sea Res.*, **12**, 323–343.

Takeuchi, K., 1984: Numerical study of the Subtropical Front and the Subtropical Countercurrent. *J. Oceanogr. Soc. Japan*, **40**, 371–381.

Uda, M., and K. Hasunuma, 1969: The eastward Subtropical Countercurrent in the western North Pacific Ocean. *J. Oceanogr. Soc. Japan*, **25**, 201–210.

White, W. B., K. Hasunuma and H. Solomon, 1978: Large scale season and secular variability of the Subtropical Front in the Western North Pacific from 1954 to 1974. *J. Geophys. Res.*, **83**, 4531–4544.